Supporting Information

Cardó-Vila et al. 10.1073/pnas.0915146107

SI Materials and Methods

Phage Display Screening and Phage Binding Assays. A random phage peptide library displaying the insert CX_7C (where X is any amino acid and C is a cysteine residue) was used for the screening; phage input was 3×10^9 transducing units (TU). Antibodies, EGF, or TGFα (R&D Systems) were coated onto microtiter wells as described (1). Briefly, 10 μg of the indicated antibodies (M225, cetuximab, 528, m-IgG, and h-IgG) dissolved in 50 μL PBS were immobilized on microtiter wells overnight at 4 °C. Wells were washed twice with PBS, blocked with PBS containing 3% BSA for 1 h at room temperature (RT), and incubated with the phage library in 50 μL PBS containing 1.5% BSA. After 2 h at RT, wells were washed 10 times with PBS, and phage were recovered by bacterial infection as described (1–3). Phage recovered on RII (second round), or on RIII for m225 panning, were used for affinity selection on cetuximab; the antibodies 528, m-IgG, and h-IgG served as controls. Purification of phage particles and sequencing of phage single-stranded (ss)DNA were performed as described (4, 5). Phage ssDNA from 96 individual clones from each of the second, third, and fourth rounds of selection were prepared, and inserts were sequenced.

Tumor Targeting. Selective phage homing to tumors was evaluated as described (4–6). Immunocompetent BALB/c female mice bearing EF43.*fgf-4* -derived breast tumors (7, 8) were deeply anesthetized and injected i.v. (tail vein) with 10^{10} TU of CVRAC-displaying phage, RGD-4C phage (positive control), and CVAAC-displaying or insertless phage (negative controls) in DMEM. Each cohort of mice ($n = 3$ per experiment) with size-matched tumors received a set of test and control phage clones. After 6 h, tumor-bearing mice were perfused through the heart with 20 mL of PBS containing 4% paraformaldehyde (PFA). Tumor and control organs were dissected from each mouse and were placed in PBS containing 30% sucrose for 24 h. Finally, tissues were frozen and sectioned at 5 μm for phage staining as described (5). For experimental therapy, BALB/c mice bearing EF43.*fgf-4*-derived tumors were established, and tumor volumes were determined as described (4, 6, 9). Treatment of tumor-bearing mice started 7 days after cell inoculation (10^5 cells/mouse).

Immunohistochemistry. Immunostaining was performed as described (10). All steps were performed at RT unless stated otherwise. Five-micrometer cryostat sections were air dried and were subsequently rinsed twice with PBS and once with PBS containing 0.3% Triton X-100 (PBST). Sections were blocked in PBST containing 5% normal goat serum (Jackson Immuno Research) for 30 min. Sections were subsequently incubated for 1 h in PBST and 1% normal goat serum containing combinations of the following primary antibodies: rabbit anti-fd bacteriophage (1:800; Sigma-Aldrich). Sections were rinsed with PBST and were incubated for 1 h in sterile PBST containing appropriate combinations of the following secondary antibodies: goat Cy3-conjugated anti-rabbit IgG (1:400; Jackson ImmunoResearch). Sections were mounted in Vectashield (Vector Laboratories). Fluorescent images were acquired with an Olympus IX70 inverted fluorescence microscope fitted with an Olympus camera and Magnafire software.

Surface Plasmon Resonance. SPR analysis was performed on a BIAcore 3000 instrument. SPR was used to determine the inhibitory effect of the peptide CVRAC or the peptidomimetic $_D$(CARVC) on the binding of the EGFR to cetuximab. A capture sensor surface was prepared by covalent immobilization of goat anti-human IgG Fc-specific polyclonal antibody (KPL) ≈500 resonance units (RU) to a C-1 sensor chip through an NHS/EDC amine coupling kit (Biacore). Binding studies were performed at a flow rate of 10 μL/min at 25 °C by equilibration of the instrument and sensor surface with the running buffer HBS-EP (10 mM Hepes, pH 7.4, 150 mM NaCl, 3 mM EDTA, 0.005% surfactant P-20). Cetuximab, diluted in running buffer (12 μg/mL), was injected over the modified sensor surface with an approximate capture of 25–30 RU. Samples containing 2.5 ng/mL EGFR in HBS-EP buffer, with or without increasing concentrations of peptides or peptidomimetics, were injected, and binding of EGFR to cetuximab was evaluated. Sensor-chip surfaces were regenerated with 50 mM NaOH. The response obtained on control surfaces (no cetuximab) was subtracted from each binding curve.

Sequence Alignment. To identify motifs resembling targeted ligands among the selected sequences, we used a peptide-matching software program based on RELIC, an established bioinformatics server for combinatorial peptide analysis and identification of protein–ligand interaction sites (11), designed and implemented through Perl 5.8.1. The program calculates similarity on the basis of a predefined amino acid window size (defined empirically and experimentally) between an affinity-selected peptide sequence and the target protein sequence from N terminus to C terminus in one-residue shifts to fit the best alignment. The peptide–protein similarity scores for each amino acid residue were calculated on the basis of an amino acid substitution matrix modified to adjust for rare residue representation. In this case, similarity scores were calculated on the basis of a five-residue window, with every pentamer motif in each selected peptide compared to each pentamer segment of the protein. Empirical similarity score thresholds were set with at least three identical residues plus one similar residue between the peptide and the protein segment.

Statistical Analysis. Student's *t* tests were used for statistical analysis of the proliferation assays. For experiments in vivo, statistical significance of the difference was computed by the Kruskal–Wallis test (nonparametric one-factor ANOVA method) with $P < 0.05$ for each treatment day. The Wilcoxon rank sum test was used to compute differences between each pairwise study group on a given day of treatment that showed statistical significance from the Kruskal–Wallis test. Statistical analysis was computed by the use of the R-Project for Statistical Computing (v. 2.4.1).

Antibodies against CVRAC peptide and ELISA. Rabbits were immunized with keyhole limpet hemocyanin (KLH)-conjugated CVRAC peptide. Purification of IgG from rabbit serum produced against the CVRAC peptide (anti-CVRAC) was performed by a standard protocol (12). Briefly, the IgG was covalently coupled to a Sepharose column and was eluted from the column with a low pH, glycine-based buffer and dialyzed against PBS.

The capacity of rabbit IgG against CVRAC to recognize CVRAC, D(CARVC), and EGFR (R&D) was measured by competitive ELISA. Plates were coated with the synthetic peptides or peptidomimetics [CVRAC, D(CARVC), D(CAAVC), CVRACGAD, CQKCDPSC; 5 μg/well] in 50 μl PBS overnight at 4°C. Subsequently, wells were blocked with 100 μl PBS containing 3% BSA at RT for 1 h. One hundred μl of the appropriate dilution of purified anti-CVRAC IgG or cetuximab was added, and incubation was continued at 37°C for 2 h. After several washes, bound antibody was detected with HRP-labeled secondary antibody (Sigma) at RT

for 1 h, followed by color development with o-phenylenediamine as a chromogen (Sigma). Absorbance was measured at 490 nm. Increasing dilutions of antisera were first incubated with constant amounts of synthetic peptides to determine the appropriate experimental range.

Synthetic peptides, peptidomimetics, or EGFR was coated onto 96-well plates at 5 μg/well. After 3 h, binding of cetuximab to the synthetic peptides was detected with an HRP-conjugated anti-human Fc antibody (diluted 1:1000; Sigma). Parallel experiments were performed to confirm that equal amounts of the synthetic peptides or peptidomimetics were bound to the plates.

For evaluation of the inhibition of binding of cetuximab to EGFR, the receptor was coated onto a microtiter-well plate and incubated with cetuximab alone or in combination with synthetic peptides or peptidomimetics. Detection of cetuximab bound to EGFR was performed as described above.

Immunoprecipitation and Western Blot Analysis. Cells were lysed in 20mM Tris-HCl (pH 7.8), 150 mM NaCl, 1mM EDTA, 1mM EGTA, 10mM DTT, 10 mM PMSF 1% Titron ×-100, phosphatase inhibitor I and II (Sigma) and protease inhibitor, sonicated, and clarified by centrifugation. For immunoprecipitation (IP) studies, lysates were incubated with primary antibodies, and the immune complexes were precipitated with protein A-Sepharose beads. Cell lysates or immunoprecipitated proteins were separated by SDS-PAGE, electro-transferred onto nitrocellulose, and probed with primary antibodies and horseradish peroxidase-labeled secondary antibodies.

For EGFR activation assays, tumor cells were starved and/or incubated with ligands. After cell lysis, co-IP with phosphorylated EGFR antibody and analysis by SDS-PAGE were performed, followed by electrotransfer to a nitrocellulose filter, the blot was probed with an anti-phosphotyrosine antibody (PY20). Signals were visualized by enhanced chemiluminescence detection (Amersham Biosciences).

Cell Viability Assays. Cells growing in 24-well plates were treated with cetuximab and the peptides or peptidomimetics as indicated for 5 days, washed twice with PBS, incubated in complete media containing MTT (500 μg/ml per well) for 2-4 h, and solubilized with 0.1 N HCl in isopropanol (13). Samples were read at 570 nm.

1. Smith GP, Scott JK (1993) Libraries of peptides and proteins displayed on filamentous phage. *Methods Enzymol* 217:228–257.
2. Giordano RJ, Cardó-Vila M, Lahdenranta J, Pasqualini R, Arap W (2001) Biopanning and rapid analysis of selective interactive ligands. *Nat Med* 7:1249–1253.
3. Cardó-Vila M, Arap W, Pasqualini R (2003) Alpha v beta 5 integrin-dependent programmed cell death triggered by a peptide mimic of annexin V. *Mol Cell* 11:1151–1162.
4. Arap W, Pasqualini R, Ruoslahti E (1998) Cancer treatment by targeted drug delivery to tumor vasculature in a mouse model. *Science* 279:377–380.
5. Pasqualini R, Arap W, Rajotte D, Ruoslahti E (2001) In vivo selection of phage-display libraries. *Phage Display. A Laboratory Manual*, eds Barbas CF, III, Burton DR, Scott JK, Silverman GJ (Cold Spring Harbor Lab Press, Cold Spring Harbor, NY), pp 1–24.
6. Hajitou A, et al. (2006) A hybrid vector for ligand-directed tumor targeting and molecular imaging. *Cell* 125:385–398.
7. Günzburg WH, et al. (1988) Expression of the oncogenes mil and ras abolishes the in vivo differentiation of mammary epithelial cells. *Carcinogenesis* 9:1849–1856.
8. Hajitou A, et al. (2001) Down-regulation of vascular endothelial growth factor by tissue inhibitor of metalloproteinase-2: Effect on in vivo mammary tumor growth and angiogenesis. *Cancer Res* 61:3450–3457.
9. Ciardiello F, et al. (1999) Antitumor activity of sequential treatment with topotecan and anti-epidermal growth factor receptor monoclonal antibody C225. *Clin Cancer Res* 5:909–916.
10. Ozawa MG, et al. (2005) Angiogenesis with pericyte abnormalities in a transgenic model of prostate carcinoma. *Cancer* 104:2104–2115.
11. Mandava S, Makowski L, Devarapalli S, Uzubell J, Rodi DJ (2004) RELIC—a bioinformatics server for combinatorial peptide analysis and identification of protein-ligand interaction sites. *Proteomics* 4:1439–1460.
12. Harlow E, Lane D (1999) Using Antibodies: A Laboratory Manual. (Cold Spring Harbor, NY: CSHL Press), pp 74–82.
13. Mosmann T (1983) Rapid colorimetric assay for cellular growth and survival: application to proliferation and cytotoxicity assays. *J Immunol Methods* 65:55–63.

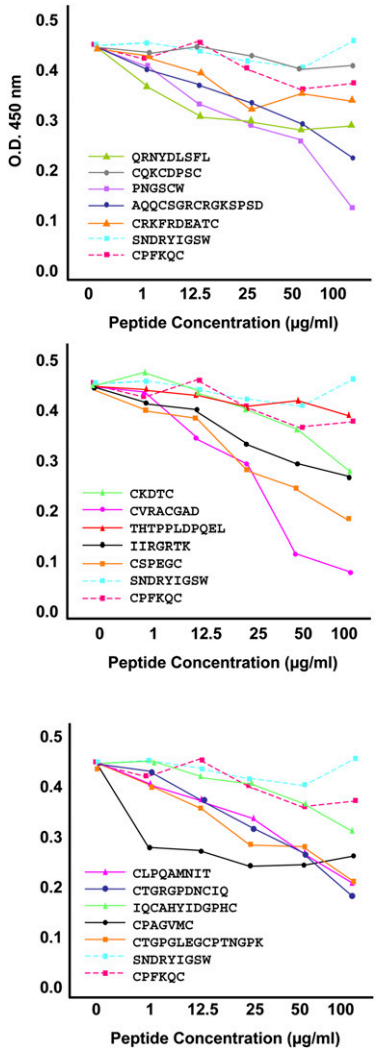

Fig. S1. Inhibition of binding of cetuximab to the EGFR by a panel of synthetic peptides. Peptides selected from the consensus motifs in all three EGFR ligands were tested for binding inhibition of cetuximab to EGFR.

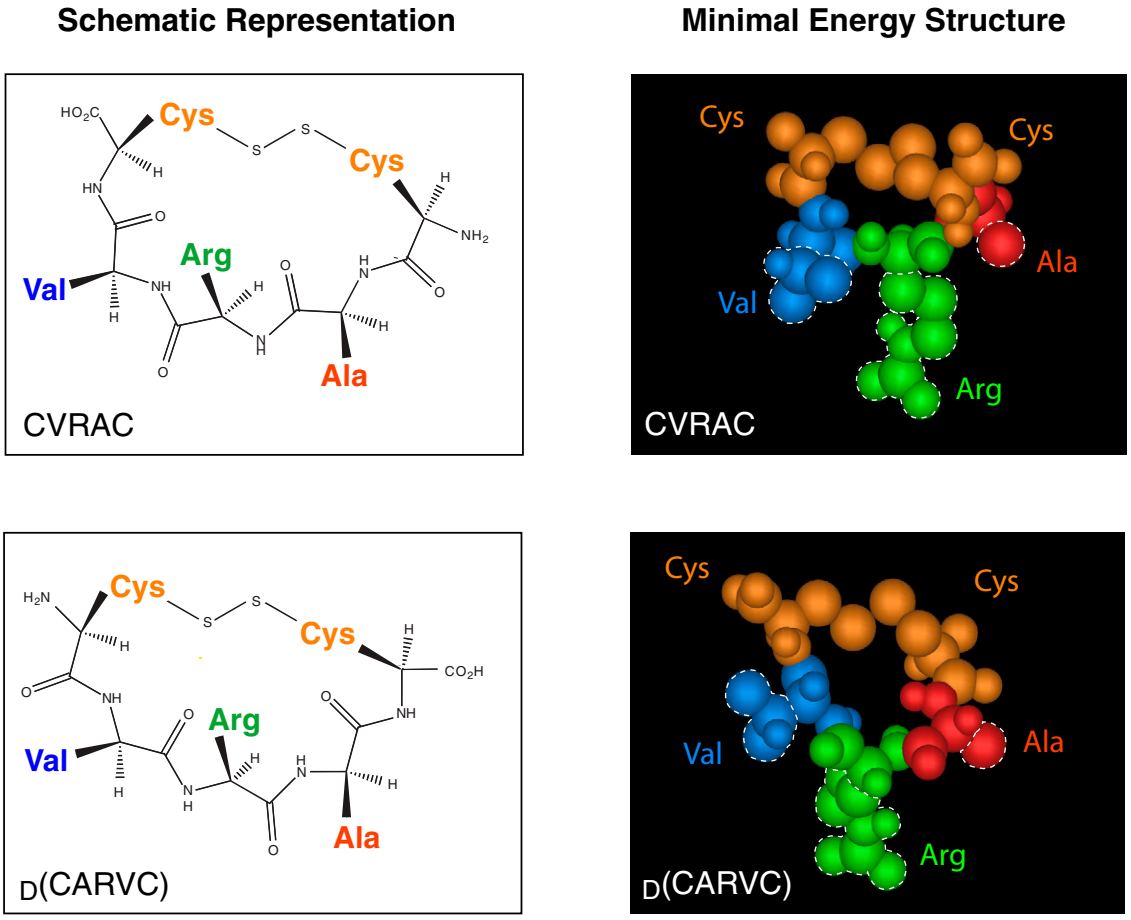

Fig. S2. Retro-inverso peptidomimetic design. Schematic representation of the retro-inverso peptidomimetic and minimal energy structure of CVRAC and $_{D}$(CARVC) is shown. Residues are color coded: cysteine (Cys, orange), alanine (Ala, red), arginine (Arg, green) and valine (Val, blue). Dotted areas indicate amino acid side chains.

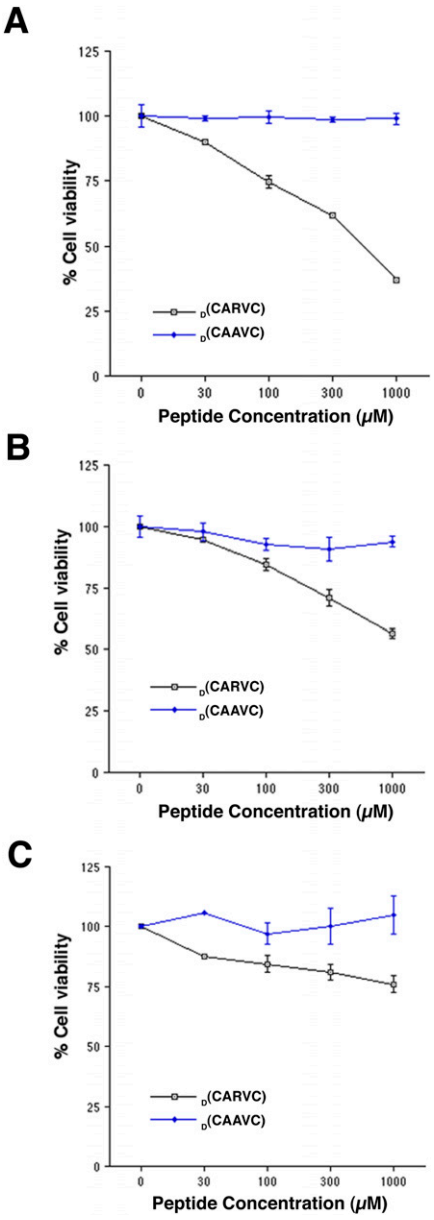

Fig. S3. Inhibition of binding of cetuximab to the EGFR on different tumor cell lines. Cells of HN5 (*A*), GEO (*B*), and EF43.*fgf-4* (*C*) were exposed to increasing concentrations of the drug $_D$(CARVC) (black line) or of the control peptidomimetic $_D$(CAAVC) (blue line). Experiments were repeated four times with similar results. A representative experiment is shown. Bars represent mean ± SEM.

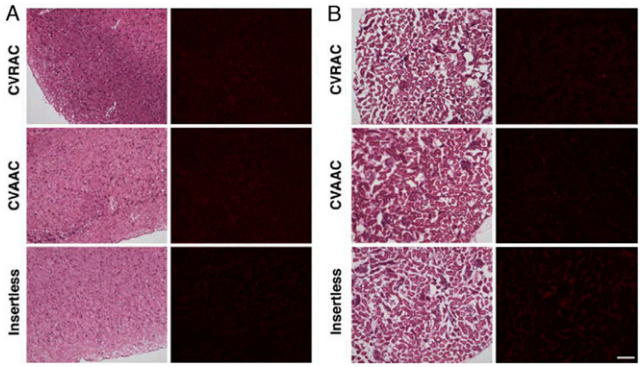

Fig. S4. CVRAC-targeted phage homes to tumor. An anti-phage antibody was used for staining. H&E staining, with the corresponding fluorescence-based immunostaining. (*A*) Brain and (*B*) kidney were used as negative control organs.

Table S1. Synthetic peptides selected from overlapping consensus motifs

Synthetic peptides	Structure	Selected on	EGFR homology region
QRNYDLSFL	Linear	EGF and TGFα	^{47}Q–L^{55}
CQKCDPSC	Cyclic	Cetuximab and TGFα	^{163}C–C^{170}
PNGSCW	Linear	Cetuximab	^{171}P–W^{176}
AQQCSGRCRGKSPSD	Cyclic	EGF and TGFα	^{191}A–D^{207}
CRKFRDEATC	Cyclic	All EGFR ligands	^{227}C–C^{236}
CKDTC	Cyclic	All EGFR ligands	^{235}C–C^{240}
CVRACGAD	Cyclic	All EGFR ligands	^{283}C–C^{290}
THTPPLDPQEL	Linear	EGF and TGFα	^{358}T–L^{368}
IIRGRTK	Linear	EGF and TGFα	^{401}I–K^{407}
CSPEGC	Cyclic	All EGFR ligands	^{486}C–C^{491}
CLPQAMNIT	Linear	Cetuximab	^{538}C–T^{546}
CTGRGPDNCIQ	Cyclic	All EGFR ligands	^{547}C–Q^{557}
IQCAHYIDGPHC	Cyclic	All EGFR ligands	^{556}I–C^{567}
CPAGVM	Linear	Cetuximab	^{571}C–M^{576}
CTGPGLEGCPTNGPK	Cyclic	All EGFR ligands	^{604}C–K^{618}